

We are IntechOpen, the world's leading publisher of Open Access books Built by scientists, for scientists

4,800

Open access books available

122,000

International authors and editors

135M

Downloads

Our authors are among the

154

Countries delivered to

TOP 1%

most cited scientists

12.2%

Contributors from top 500 universities



WEB OF SCIENCE™

Selection of our books indexed in the Book Citation Index
in Web of Science™ Core Collection (BKCI)

Interested in publishing with us?
Contact book.department@intechopen.com

Numbers displayed above are based on latest data collected.
For more information visit www.intechopen.com



The Evaluation of Asphalt Mixture Mastic as an Aging Indicator

Carlos Alfonso Cuadro Causil, Wilmar Darío Fernández-Gómez, Jorge Iván Osorio Esquivel and Fredy Alberto Reyes Lizcano

Abstract

This chapter studies two mastic rheological properties after aging processes. The former is mastic produced in the laboratory, and the latter is the one extracted from asphalt pavements in service. A Colombian asphalt cement of two penetration grades was used to mix laboratory mastics, and two fillers were used also. Field mastics were extracted from in-service asphalt pavements constructed with the same asphalt mixture. Laboratory mastics were submitted to varying accelerated aging treatments in the laboratory, rolling thin-film oven (RTFO) test and an ultraviolet (UV) radiation chamber, to short- and long-term aging, respectively. Rheological measurements with a dynamic shear rheometer (DSR) were developed and calculated the aging master curves based on the rheological models. The results show the progression of hardening in the laboratory mastics as well as field mastics. In summary, mastic analysis is going to be a good indicator of the asphalt mixture aging.

Keywords: aging, rheology, mastic, SHRP aging, UV radiation

1. Introduction

Highway pavement asphalt is affected by the presence of oxygen, UV radiation, and temperature changes. Taken together, these three aging aspects appear throughout the production of the asphalt mixture, construction of the road, and service life. Asphalt's aging variables could be classified as either intrinsic or extrinsic. While the former refers to the volatilization of lightweight fractions, oxidation (oxygen absorption and diffusion), thixotropy, syneresis, and degradation of the polymeric structure (in the case of modified asphalts), the latter refers to the mixture's air void content, binder's film thickness, transit and thermal wear, as well as the aggregate type and filler proportions (filler minerals or fine materials). An undoubtedly complex phenomenon, asphalt aging, has consequences ranging from reduced durability to changes in the asphalt's physicochemical properties and chemical composition [1].

The production, storage, transport, and laying of asphalt mixtures cause compositional changes, i.e., changes in the mixture's physicochemical properties; these changes are also found in the asphalt mixture employed as road pavement [2–4]. However, the majority of design models for asphalt mixtures only focus on one of the “unaged” asphalt's physical properties. Moreover, within the variables and considerations, these models utilizing temporal changes in asphalt properties are not taken into account [5].

Not only it is faced with the difficulty concomitant to ensuring satisfactory yield from mixtures after the aggregates are added to the asphalt, but it must account for the incredible demand placed upon this mixture by long-term transportation. It is incumbent upon us, then, to employ laboratory techniques in a timely, cost-efficient manner to study the aging behavior of asphalt mixtures. Such techniques would ideally require the minimal amount of material for analysis. Consequently, mastics before the start of their service life were examined. Considering that the present data in the case of asphalt aging via mastic analysis is relatively scarce (in comparison to that of asphalt mixtures in general), this study contributes new data: the effect of mastics in the long-term aging of asphalt mixtures.

The physicochemical properties of mastic directly and significantly influence the performance of asphalt mixtures based on the type of filler mineral used and the relative proportions of the mixture itself—variables which could factor heavily in the mixture's resistance to aging. This research aims to fill the gap in knowledge with regard to the effect of filler minerals on the long-term aging of asphalt binders [5].

The efficacy of basing predictions for asphalt mixture behavior on mastics by way of a rheological analysis of the latter using laboratory-aged asphalt mixture samples developed with Colombian ACs 60-70 and 80-100. This project, then, addresses the need for the development of an asphalt aging index (AI) based on the rheological analysis of mastics. To do so, both field and laboratory samples were analyzed. In sum, the benefit of mastic analysis lies in that it allows to construct master curves and predict the asphalt mixture aging.

The specific objectives of this project are as follows:

Employ rheological analyses on mastics produced in the laboratory.

Construct master aging curves with the data obtained from asphalt mastics in the field.

Propose a linear viscoelastic model of asphalt mixture behavior that has a quadripartite scientific foundation: the linear viscoelastic model, the effect of aging, the aging master curves, and the aging shift factor.

1.1 Mastic

In general, hot-mix asphalt (HMA) is composed of aggregate minerals, asphalt binder, and air voids. Insofar as the mastic is concerned, it is composed of binder and filler minerals (mineral aggregate put through a Sieve #200 or less than 75 μm). The fillers' mineral components play a crucial role in both the mastics' and the HMA's properties as they can diminish the aging effects by virtue of increased viscosity [6–8]. Therefore, a thorough understanding of the fillers in both the mastic and the HMA proves to be invaluable for developing high-performance, well-designed asphalt [9–12].

Various studies on the rheological properties of asphalt mastic and other types of filler highlight the diversity of mineral fillers used, in addition to identifying the reinforcement they provide when added to asphalt cement. The consensus reached is that these fillers influence the physicochemical interactions within the mixture itself; in other words, filler is more than some inert substance used to fill holes between thick aggregate particles in the asphalt mixture. In fact, it is an active material whose activity occurs in the interface between the applied load and the asphalt binder [13]. Although Lesueur and Little [14], Hopman et al. [15], and Buttler [8] have documented the aforementioned interactions, the role of fillers in asphalt mixtures is sufficiently complex so as to require further study.

1.2 Viscoelasticity

In a viscoelastic material, the relationship between stress and deformation depends on the weight and speed of the load applied. When materials of this type are faced with a load, they present a characteristic relaxation time that corresponds to the amount of time each material takes to restructure itself and achieve equilibrium. Due to the fact that each viscoelastic material has its own relaxation time dependent upon temperature and load application, a temperature increase translates into faster structural readjustment (i.e., temperature reduces relaxation time). Therefore, we can induce any material to reach the same relaxation time with either a quick high-temperature or a slow low-temperature treatment.

Myriad asphalt studies have observed its viscoelastic nature and concluded that fundamental rheological methods should be employed to obtain proper material characterization. Unfortunately, few have had the necessary resources and sufficient background to study asphalt films (binders) by way of rigorous rheological methods [16]. The characterization of the viscoelastic properties of asphalts uses a rheometer with cone and plate geometry, which measures the complex moduli of aged and unaged asphalts over a wide array of temperatures and frequencies. As a result, these studies hypothesize that oxidation changes the temperature dependence of the material and that these changes tend to increase as temperature increases [17]. Dickinson and Witt [18] later confirmed these findings.

1.3 Aging

Aging is usually quantified in the form of an Aging Index (AI), whether directly or indirectly. These aging indices have been especially popular in regard to the quantification of long-term aging (service life). A single AI point portrays the relation between aged and unaged asphalt viscosities, as well as describes increased hardening when the asphalt's response is essentially viscous. The problem here is that this single point does not offer an exact reflection of the changes in rigidity at low temperatures when the phase angle provides a significant portion of the response [19]. In 1981, Vallerga et al. used UV radiation and infrared lights to age asphalt binders. UV radiation turned out to be an extremely effective method—in empirical terms—of changing the asphalt's softening point, ductility, and penetration after oxidation had occurred; similar results were obtained by Fernández et al. [3].

1.4 Time-temperature superposition and master aging curves

As it has been mentioned, the behavior of viscoelastic material depends on temperature and load frequency: a viscoelastic material subject to high-frequency loads at low temperatures behaves the same as one subject to low-frequency loads at high temperatures. A change in temperature modifies the distribution of relaxation times such that all times corresponding to a distribution obtained at a temperature (T_d) are related to the corresponding times of another distribution obtained at a different temperature (T). Thus, relation between the two relaxation times corresponds to the respective temperatures.

The dependence a_t on temperature is expressed by the Williams-Landel-Ferry (WLF) equation:

$$\text{Log}a_T = \frac{-C_1(T - T_d)}{C_2 + T - T_d} \quad (1)$$

where $a(T)$ is the aging shift factor, T is the aging time for the present study, T_d is the reference aging time for the present study, and C_1 and C_2 are the empirical

constants. In light of the correlation between aging effects and temperature, it developed the master aging curves similar to the master temperature curves by shifting the experimental data horizontally. Given that the rheological properties include the complex moduli and the phase angles, two master curves were needed to adequately describe the material's behavior [5].

Analysis of the shift factor in SHRP aged and unaged asphalts carried out by the authors of this study shows that the constants for the WLF equation can essentially assume the same values: -19 for C1 and 90 for C2. These values concur with those previously obtained by other authors [20], where the amount of shift required for each temperature to form the master curve is especially important and is referred to as the shift factor $a(T)$. A graph $\text{Log } a(T)$ against temperature is normally prepared in conjunction with the master curve. Such a graph visually indicates how the viscoelastic properties of the materials change with temperature.

Applying the principle of time-temperature superposition (TTS) to the construction of master curves, in addition to determining the shift factor, proves to be a powerful investigative tool that clearly outlines the time and temperature dependence of asphalt cements [21]. The temperature dependence in asphalt cements, in terms of the variation of $\text{Log } a(T)$, is a function of time, and it can be mathematically modeled using the WLF equation at high temperatures.

Aging time data shifts with respect to the logarithm of time until the curves converge to form a single smooth one. The resulting master aging curve moduli describe the dependence of the material on aging time. The amount of shift for each aging time required for the master curve describes the material's dependence on aging time; the logarithm of the aging shift factor is the shift undergone by the complex moduli in relation to a given reference aging time (to form a single curve). The reference aging time to construct the master aging curve can be arbitrarily chosen [5].

1.5 Linear viscoelastic model

Asphalt's viscoelastic nature has led to a variety of ways to interpret the behavior of natural asphalts and asphalt mixtures. The models proposed range from the empirical (also known as mathematical or phenomenological models), e.g., Jongepier and Kuilman [22], Dobson, [23], Dickinson and Witt [18], Christensen and Anderson [21], Stastna et al. [24], Marasteanu and Anderson [25], Zeng et al. [26], Elsefi et al., and Mohammad et al. [27], to the mechanical (based on rheology), e.g., Huet [28], Huet-Sayegh model [29], Olard and Di Benedetto [30], and Di Benedetto and Neifar [31]. The former set of models tries to predict the behavior of the viscoelastic material using master curves that combine complex modulus and phase angle behavior within a wide range of frequencies and temperatures. In contrast, the latter set of models takes into account the material's linear and nonlinear behavior. In general, these models are capable of predicting the linear viscoelastic properties by employing the TTS principle. For a detailed description of the different models, see Yusoff et al., [32].

2. Materials and methods

2.1 Materials

Two types of mastics were evaluated for this project: the first was developed in the laboratory, and the second was extracted from field pavements. The laboratory mastics were made with an asphalt cement (AC) of two penetration grades most commonly found in Colombia, AC-60-70 and AC-80-100, from the Ecopetrol Refinery

located in Barrancabermeja, Colombia; they contain a fine material produced by the trituration of alluvial material and in proportions of 2, 10, and 20% of the mixture's total weight. From the combination of the two asphalt cements and the three proportions of fine material, six distinct samples were obtained (identified in **Tables 1–3**).

To determine the rheological characteristics of the two asphalts, a TA Instruments dynamic shear rheometer (DSR) AR 2000 EX was used. The evaluation yielded results according to the performance grade (ASTM D6373-07) for medium to high temperatures; **Tables 2** and **4** display those results. Asphalt characterization was led to classify both as PG 58 for high temperature and 16 for medium temperature; low temperature was not measured because pavements in Colombia are not exposed to temperatures below 0°C (**Table 5**).

The FTIR spectroscopy allowed us to map the effects of UV radiation on the asphalts studied. Due to the low sensibility concomitant to FTIR spectroscopy in macromolecules like asphalts, we used the oxidants H₂O₂ (30% v/v) and HNO₃ (63% w/v) to help identify functional groups C=O or S=O. Due to the low sensibility concomitant to FTIR spectroscopy in macromolecules like asphalts, we used the oxidants H₂O₂ (30% v/v) and HNO₃ (63% w/v) that help us to identify on the functional groups the magnitude of strong oxidation C=O or S=O. The oxidants mixed with original asphalts AC-20 and AC-30 for 48 h were tested by infrared

Sample	Code
AC-60-70 + 2% filler mineral	1
AC-60-70 + 10% filler mineral	2
AC-60-70 + 20% filler mineral	3
AC-80-100 + 2% filler mineral	4
AC-80-100 + 10% filler mineral	5
AC-80-100 + 20% filler mineral	6

Table 1.
 Laboratory samples.

Experiment	Method	Unit	AC-60-70
Original binder			
Penetration (25°C, 100 g, 5 s)	ASTM D-5	0.1 mm	63.4
Specific weight	INV. E-707	—	1.012
Penetration index	NLT 181/88	—	0
DSR viscosity (60°C)	ASTM D-4402	Pa s	145.6
Ductility (25°C, 5 cm/min)	ASTM D-113	cm	>105
Softening point	ASTM D-36-95	°C	52.4
Solubility trichloroethylene	ASTM D-2042	%	>99
Water content	ASTM D-95	%	<0.2
Flash point	ASTM D-92	°C	323
Residue RTFO test binder			
Mass loss	ASTM D-2872	%	0.3
Penetration (25°C, 100 g, 5 s)	ASTM D-5	0.1 mm	62

Table 2.
 Physical characterization of AC-60-70.

Experiment	Method	Unit	AC-80-100
Original binder			
Penetration (25°C, 100 g, 5 s)	ASTM D-5	0.1 mm	83.2
Specific weight	INV E-707	—	1.007
Penetration index	NLT 181/88	—	0.3
DSR viscosity (60°C)	ASTM D-4402	Pa s	136
Ductility (25°C, 5 cm/min)	ASTM D-113	cm	>105
Softening point	ASTM D-36-95	°C	50.5
Solubility trichloroethylene	ASTM D-2042	%	>99
Water content	ASTM D-95	%	<0.2
Flash point	ASTM D-92	°C	358
Residue RTFO test binder			
Mass loss	ASTM D-2872	%	0.5
Penetration (25°C, 100 g, 5 s)	ASTM D-5	0.1 mm	61

Table 3.
Physical characterization of Colombian AC-80-100.

Temp.	Delta	G*	(G*/Sin δ)	(G*Sin δ)
°C	°	kPa	kPa	MPa
Original				
52	84.52	4.76	4.78	
58	86.18	1.90	1.90	
60	86.61	1.46	1.46	
64	87.40	0.82	0.82	
RTFO				
52	81.24	5.25	5.31	
58	82.10	3.98	4.02	
60	83.52	2.30	2.32	
64	85.38	1.09	1.09	
76	86.76	0.52	0.52	
PAV				
13	42.09	12.00		7.97
16	45.40	7.01		4.84
19	48.09	4.78		3.43
22	54.39	2.96		2.21

Table 4.
Partial performance grade for AC-20 (60-70).

spectroscopy and allowed us to identify changes in carbonyl and sulfoxide groups. The results shown in **Figure 1** exhibit significant increases in the 1650 cm^{-1} band, the domain of functional carbonyl groups, which indicates the oxidation of carbon atoms. We found minimal sulfoxide variations after oxidation, a situation

Temp.	Delta	G*	(G*/Sin δ)	(G*Sin δ)
°C	°	kPa	kPa	MPa
Original				
52	86.00	4.31	4.32	
58	87.22	1.81	1.81	
60	87.64	1.35	1.36	
64	88.09	0.91	0.91	
RTFO				
52	82.28	9.08	9.16	
58	84.32	3.90	3.91	
60	85.04	2.88	2.89	
64	85.98	1.72	1.72	
76				
PAV				
10	39.62	18.87		12.03
13	42.09	13.06		8.75
n16	45.40	6.83		4.87
19	48.09	4.84		3.60
22	54.39	2.58		2.10

Table 5.
 Partial performance grade for AC-20 (80-100).

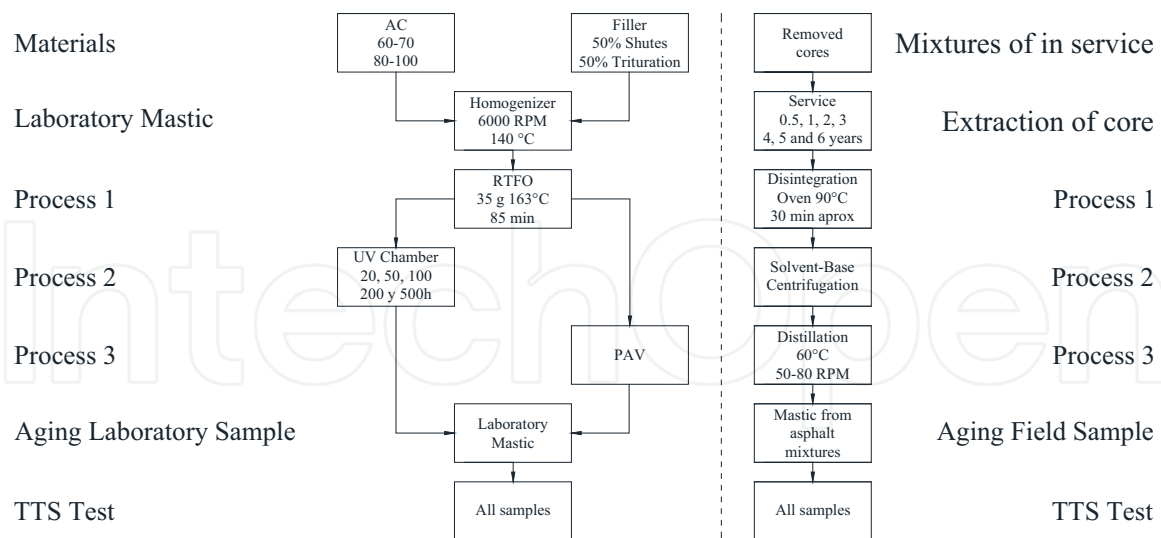


Figure 1.
 FTIR spectra of original asphalts AC-30 and AC-20 (left) and AC-30 and AC-20 after 48 hours of oxidizing agent exposure (right) [33].

that leads us to propose that “unaged” asphalts exhibit S=O groups as a result of the previous aging brought about by extraction and refinement. **Figure 1** also allows us to compare the oxidation achieved by strong oxidants and that of the UV chamber [33].

In order to show an outline of the methods at this project, **Figure 2** plots an outline of this.

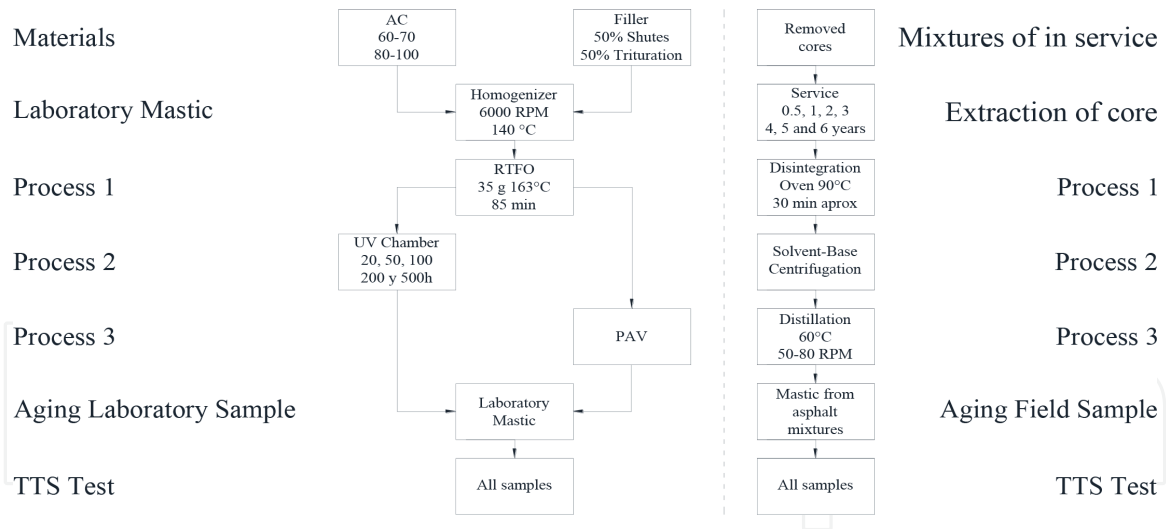


Figure 2. Methodology outline [34].

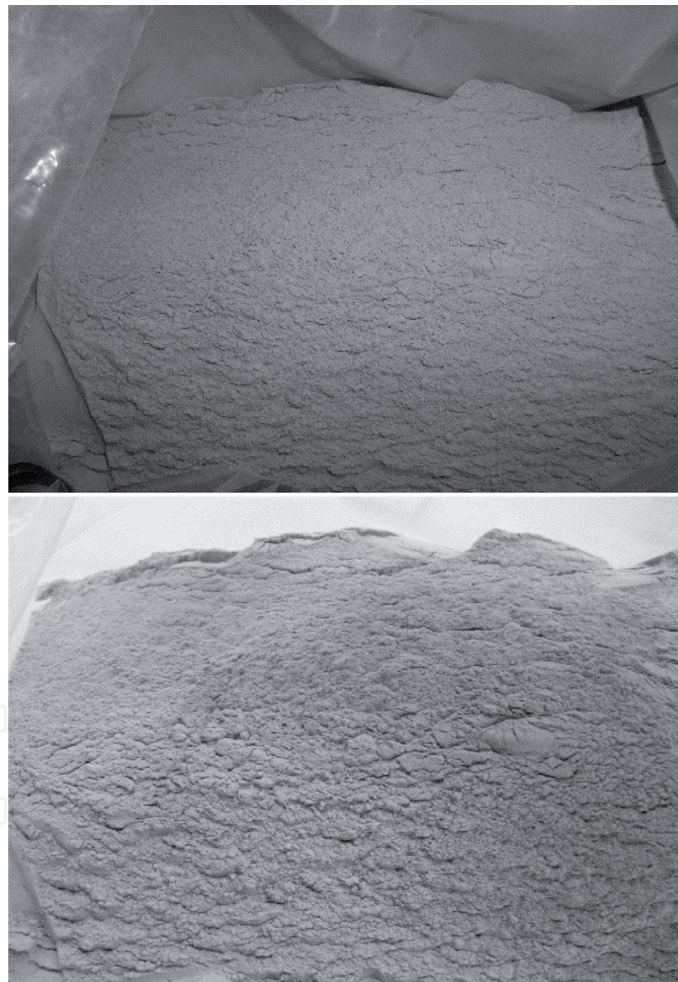


Figure 3. Filler aggregate (above) and chute aggregate (below).

The filler mineral is an aggregate from the Coello River in Tolima, Colombia. The filler was obtained by a mixture of 50-50 split between two sources: the first taken from the aggregate trituration plant and the second from the asphalt plant's chutes. **Figure 3** shows two different fillers. Before mixing the two materials, both are passed through a Sieve #200 (75 μ m). After, the field mastic was extracted from flexible pavements used in Bogota's roads, with service life ages of 12, 24, 60, and 72 months. In order to obtain these field samples, a core of the asphalt binder



Figure 4.
Yamato BO600 rotary evaporator.

under study was extracted and brought to the laboratory. Thus, it can ensure that field mixture possesses the same gradation characteristics and asphalt content as that produced in the laboratory.

To fabricate laboratory mastic, the materials were heated at 140°C in a ventilation-free oven. The mixture is then produced with a HDD ULTRA TURRAX-T50 BASIC homogenizer for 5 minutes at a constant temperature of 140°C at 6000 rpm. The mixtures were stored in hermetic metal containers until tested. Once obtained, the fine asphalt mixture aggregate (the mastic) undergoes short- and long-term aging treatments. In the case of short-term treatment, a rolling thin-film oven (RTFO) Model CS 325-B manufactured by James Cox & Sons, Inc. was used for 85 minutes at 163°C. For the long-term aging treatment, the mastic was exposed to UV radiation in an aging chamber—ultraviolet ATL-360—that was built for this project following the standards established by ASTM D4799-08. Each exposure period consists of a 2-hour radiation cycle followed by a 2-hour condensation period, so that the mastic is subjected to continuous exposure periods of 20, 100, and 500 hours.

In order to recover the mastic from the asphalt mixtures of in-service pavements, cylindrical cores 10 cm in diameter and on average 10 cm thick were removed. Subsequently, disintegration, centrifugation, and solvent-based distillation of the core samples were carried out. The disintegration process consisted of heating the cores to 90°C for 40 minutes in a BLUE LINE OV 12A oven before gently separating the aggregates mechanically. The centrifugation was performed with a HOUGHTON MFG E2 centrifuge, using 800 g of asphalt mixture and 900 ml of solvents (70% toluene and 30% ethanol by volume). Centrifugation successfully achieved a mixture of solvents and mastics for each core sample. As far as distillation is concerned, the mixtures were placed in a Yamato BO600 rotary evaporator at a speed ranging from 50 to 80 rpm and with a temperature of 60°C. **Figure 4** shows the rotary evaporator. The entire distillation process takes approximately 30 minutes. Finally, the resultant mastic is left to “air out” for 3 days to facilitate the evaporation of the residual solvent and stored in hermetic metal containers until rheologically evaluated.

For both the laboratory and field samples obtained via the process outlined, the rheological evaluation of the materials was done with the DSR TA INSTRUMENTS AR-2000 EX's rheological testing. Tests were addressed on 25 mm geometry with a gap of 1000 μm at temperatures of 15, 25, 35, 45, 55, and 65°C. Taken together, this

information and the TTS principle allow us to create master curves for behavior at a temperature of 25°C according to the aging shift factors produced by the CAM and WLF models.

2.2 UV radiation of the mixture

The samples were submitted to UV radiation in an aging chamber that has eight lamps. These lamps emit radiation with a wavelength of 340 nm in the range of UVA rays. **Figure 5** shows the aging chamber. Exposure times for the mastic samples analyzed varied between 0 and 500 hours to reflect conditions encountered in the field. In other words, if Bogota’s average integrated solar radiation—measured in a wavelength of 340 nm—is 2.2 W/m² nm per day (IDEAM, 2005), we can extrapolate that figure to estimate an annual UVA exposure of 8.8 or 3155 kJ/m². Therefore, the aging chamber’s radiation value of 1.55 W/m² nm per cycle (ASTM G 154-06) meant we had to put the mastic samples through 500 hours of UVA radiation to simulate a year of exposure in the field as pavement in Bogota (see **Table 6**). Within the chamber itself, we placed 2-mm-thick mastic samples on two 300-cm rectangular plates (10 cm wide and 3 mm deep).

The mastics were treated in the UV chamber’s 4-hour cycles of radiation and condensation (as it has been previously stated, each cycle consists of 2 hours of radiation followed by 2 hours of condensation). The 2-hour condensation period exposed the samples to a temperature of 60°C at 99% humidity, since these conditions reflect Colombia’s tropical climatic conditions. Moreover, they recreate conditions propitious for asphalt oxidation. Alternating between the two periods emulates what the materials face in the field. That is to say, after diurnal UV exposure, there comes a nocturnal “rest period” during which the



Figure 5.
Aging chamber.

UVA exposure period (hours)	Equivalency (months)
50	1.2
100	2.4
200	4.8
500	12

Table 6.
Exposure to UV radiation and months in the field equivalency.

reactions that determine the physical and chemical changes of the material occur [35]. The samples treated in the aging chamber were analyzed with the DSR to establish the changes exhibited by the asphalt—the difference between unaged and aged samples.

2.3 Time-temperature superposition test

The TTS test provides dynamic material testing over a number of frequencies at different temperatures. Owing to the fact that temperature corresponds to the linear viscoelastic region of the material, these curves are parallel, and the shift factor responds to the curve's horizontal shift toward a reference temperature at each given temperature (in this case, 25°C). This test essentially made use of the same

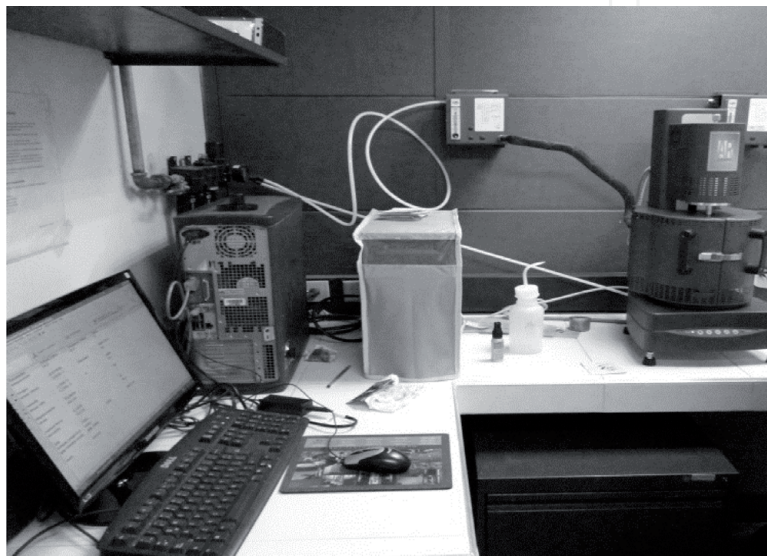


Figure 6.
DSR TA Instruments AR-2000 EX.

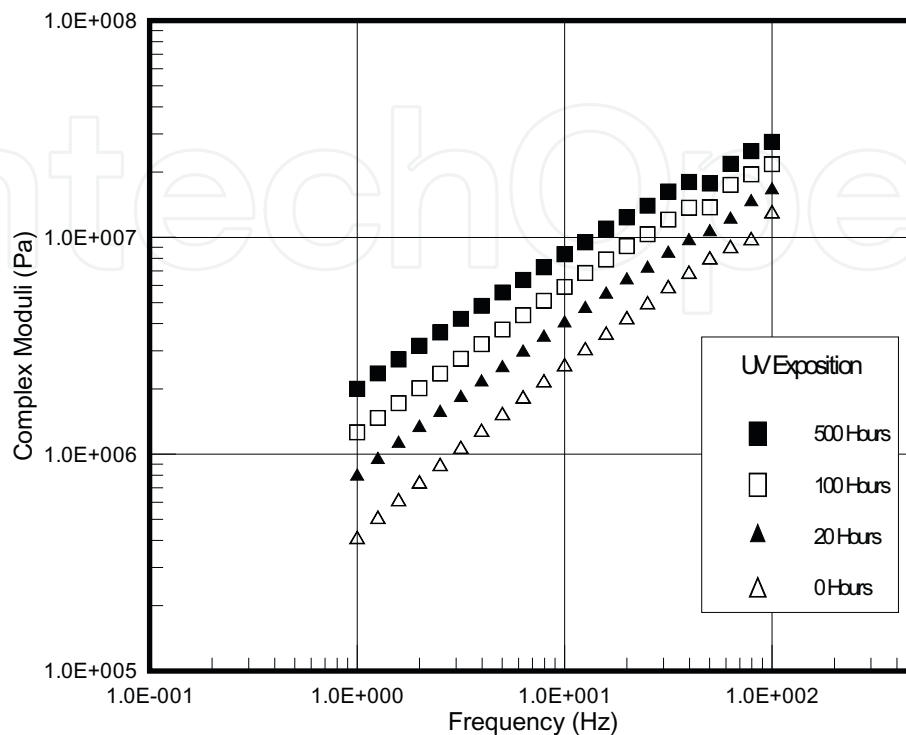


Figure 7.
Complex moduli ($|G^*|$) of sample 1 after various exposure periods.

principle: instead of different temperatures, different aging periods were taken into account to obtain the aging shift factor for each sample.

The range of frequencies covered is from 1 to 100 Hz and that of temperatures is 25, 35, 45, 55, and 65°C. This investigation used a deformation percentage of 0.2% since mastic may present more hardening than the aged asphalt, and in order to ensure fidelity to the data over the linear viscoelastic region, those evaluations were performed with dynamic shear rheometer AR-2000 EX (**Figure 6**). From this information, master aging curves following the WLF model were created. The reference temperature was 25°C, and the curves' shift factors for four aging levels corresponding to 0, 20, 100, and 500 hours, respectively, were obtained. The graph below (**Figure 7**) displays the behavioral curves for the complex moduli of the AC-60-70's mastic with 2% of fillers at different stages of aging in the UV chamber. The same methodology was employed to construct the master curves for all six laboratory samples.

With the information gained from the TTS test, aging master curves were plotted using the modified CAM model, where empirical algebraic equations are employed for modified asphalts and asphalt mixtures under a dynamic load of low shear stress in a wide range of frequencies, temperatures, and deformations. The model is composed of four formulations for the master curves of $|G^*|$ and δ . Thus, equation simulates the behavior of the mastic both as a viscoelastic fluid and as a solid. The equation of the $|G^*|$ is rooted in a generalization of the CAM model and the universal model. Below, the reader will find the equations for the $|G^*|$:

$$|G^*| = G_e + \frac{G_g - G_e}{\left[1 + \left(\frac{f_c}{f}\right)^k\right]^{\frac{m_e}{k}}} \quad (2)$$

where $G_e = |G^*|(f \rightarrow 0)$ with $G_e = 0$ for mastic; $G_g = |G^*|(f \rightarrow \infty)$; f_c is a positional parameter with frequency dimensions; f is the reduced frequency, a function of temperature and deformation; and k and m_e are dimensionless parameters.

3. Results and discussion

3.1 Aging master curves for the complex moduli in the laboratory

Because rheological properties encompass the complex moduli and phase angles, we were obligated to develop two master curves to properly describe the material's behavior. Here, it is necessary to emphasize that this research saw an increase in temperature that mirrored a decrease in aging time. Similar results have been reported [5]. The resulting shift is the aging master curve for the six samples presented in **Figure 8**.

As a result of our aging master curves, various shift factors were obtained; based on these factors, the empirical constants for the WLF model and the variables for the CAM model were calculated. The margin of error for the calculated empirical constants was less than 6%. The CAM model variables, the WLF empirical constants, and their correlations in all of the samples are summed up in **Table 7**.

Results were consistent with those of other studies insofar as the increase in aging time parallels that of the complex moduli as a factor in aging; for example, Huang [5] reports that increasing the level of aging time, the complex modulus increases. On the other hand, this author assumed E^* (MPa) = 0 and $m = 1$ [5], in this investigation those variables were calculated, and our results are 0.0105 and 1.09, respectively.

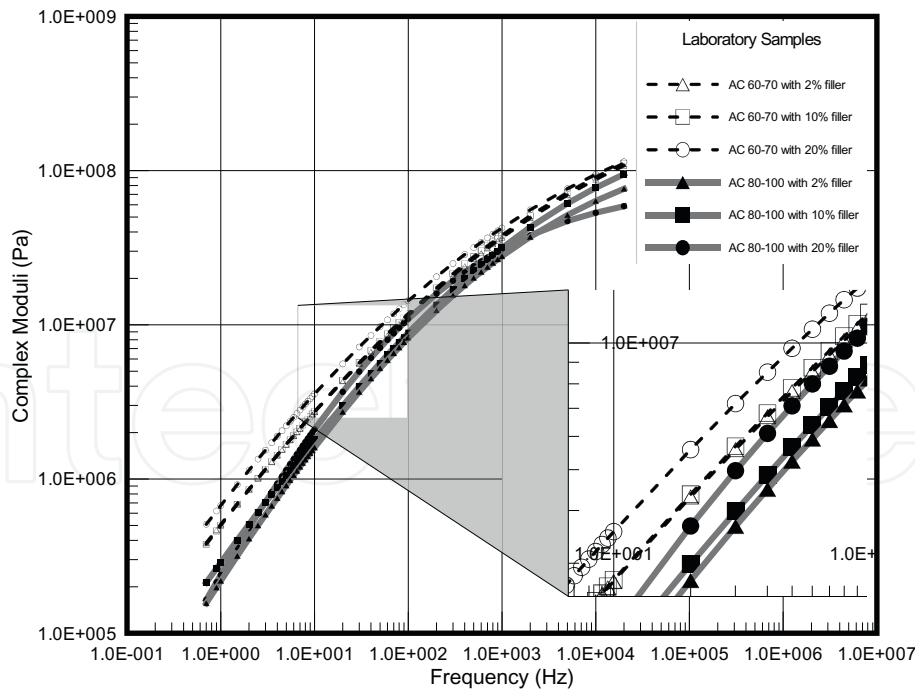


Figure 8.
 Aging master curves for the six laboratory samples.

Sample	E^*e (MPa)	E^*g (MPa)	f_c	k	m_e	R^2	C_1	C_2	R^2
1	0.011	424.03	220.32	0.22	1.04	0.995	0.85	53.30	0.987
2	0.011	424.03	180.45	0.22	1.03	0.995	0.75	17.06	0.988
3	0.013	427.03	157.05	0.23	1.02	0.987	0.86	59.61	0.940
4	0.002	201.68	191.99	0.28	1.14	0.995	0.78	126.24	0.943
5	0.010	267.45	154.30	0.26	1.17	0.996	0.80	119.71	0.993
6	0.001	82.34	81.35	0.39	1.21	0.994	0.71	17.98	0.999
Field	1.118	424.03	2.20	0.23	1.04	0.954	10	66.57	0.695

Table 7.
 CAM and WLF constants.

Evidence of the aging dynamic is presented in **Figure 9**. This graphic charts the aging shift factor against aging time for each sample. The increase in shift factor as it relates to time could clearly identify. However, it must point out that the time presented corresponds to a long-term aging treatment. Therefore, the time scale can be interpreted in hours for laboratory aging or months in service life, as the equivalences in **Table 6** demonstrate. A logarithmic regression done with the R^2 coefficient was 0.75; this means that environmentally aged mastic can increase their complex modulus after 500 hours.

To validate the viscoelastic model, we refer readers to **Figure 10**, in which graphs of the complex moduli are measured against predictions. Strong correlation between the predicted and measured complex moduli was found (0.99).

The aging dynamic of the aging shift factor indicates aging. Hence, regressions can be used to predict the complex moduli that samples would present after 1000 hours of aging in the UV chamber. Nevertheless, the physical hardening present after aging depends on the aging shift factor and the slope of master curve in the linear viscoelastic region. From the CAM model, the m_e factor obtained corresponds to this slope. Readers can find the physical hardening (i.e., aging index) factors—especially as they relate to the aging shift factor for the mastics analyzed—in **Tables 8 and 9**.

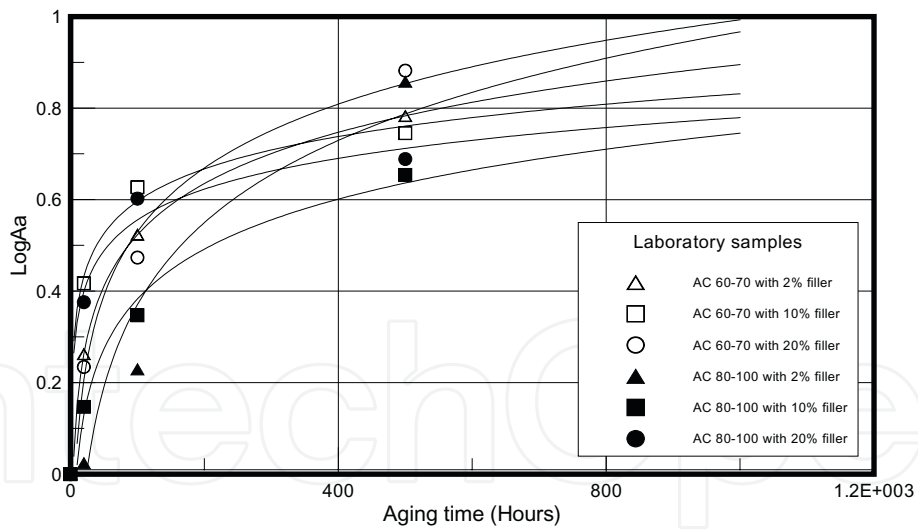


Figure 9.
Aging shift factors.

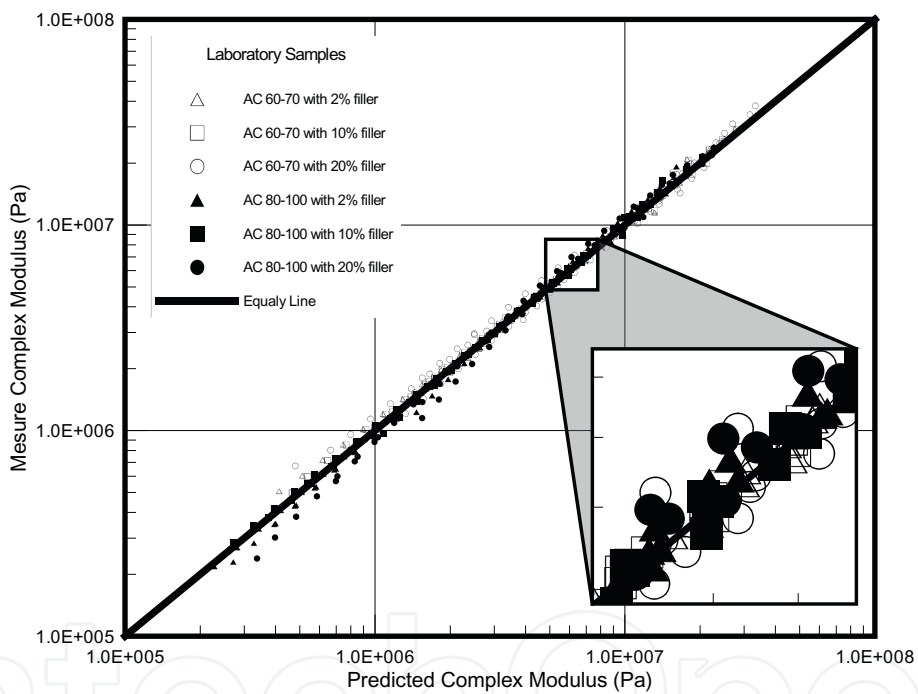


Figure 10.
Predicted versus measured complex moduli.

Age (h)	AC-60-70					
	ASF S-1		ASF S-2		ASF S-3	
	AI	AI	AI	AI	AI	AI
me	1.04		1.03		1.02	
0	0	0	0	0	0	0
20	0.26	0.27	0.42	0.43	0.23	0.24
100	0.52	0.54	0.63	0.65	0.47	0.49
500	0.78	0.81	0.75	0.78	0.88	0.92

Source: Authors.

Table 8.
Mastic aging index AC-60-70.

AC-80-100						Field samples	
ASF S-4	AI	ASF S-5	AI	ASF S-6	AI	Age (years)	AI
1.14		1.17		1.21		1.04	
0	0	0	0	0	0	1	0.00
0.02	0.02	0.15	0.15	0.38	0.39	2	0.18
0.23	0.24	0.35	0.36	0.60	0.63	5	0.35
0.86	0.89	0.65	0.68	0.69	0.72	6	0.91

Table 9.
 Mastic aging index AC-80-100 and field samples.

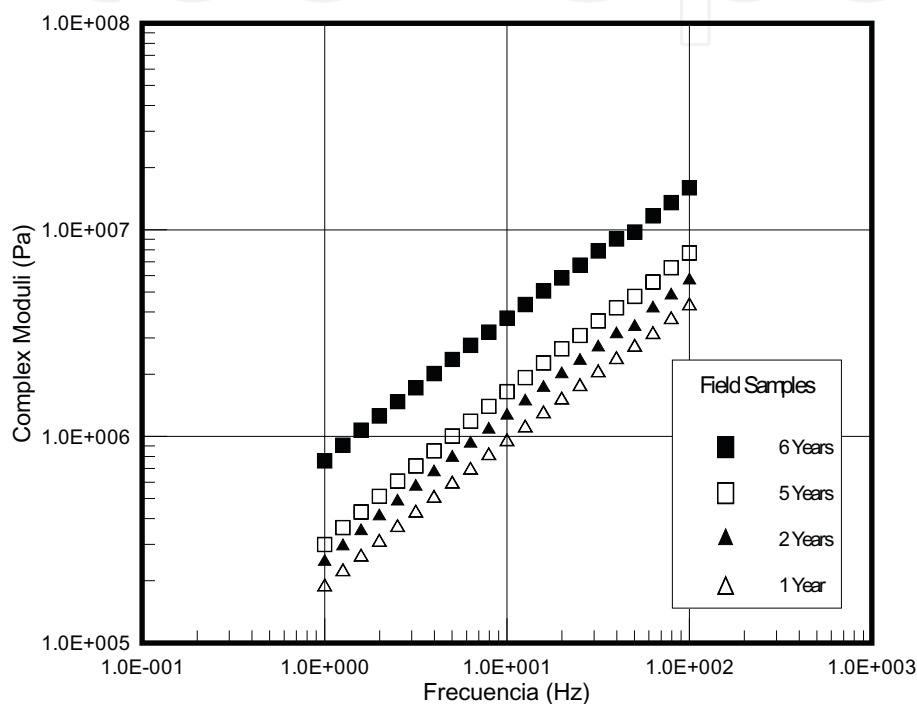


Figure 11.
 Master curves for the complex moduli at 25°C.

3.2 Master curves for the complex moduli of field samples

The procedure used for the laboratory samples was also applied to the field samples. **Figure 11** charts the complex moduli of the field samples' master aging curves at different stages of service life.

If AI values superimpose on the data gleaned from the laboratory mastic, an acceptable correlation cannot be traced, perhaps due to the fact that the field mastic contains filler that solvent mixtures were unable to verify. Although behavior of 20% content fine's material is a good representative to field samples because correspond to average observed for those samples, future expectative research to correct this situation. Nonetheless, upon observing that the aging shift factor values approach 1 after 1 year of service life, we can state that the material exhibits its maximum hardening values, which do not increase substantially over time.

4. Conclusions

The rheological analysis of mastics allows us to predict aging in asphalt mixtures. The WLF equation for the temperature dependence of the complex moduli

helps model mastic aging levels for Colombian asphalts 60-70 and 80-100, as it also does for the proportions of filler present in the mixture. The WLF model draws parallels between temperature and aging behavior: they have inverse proportions, with a decrease in temperature stimulating an increase in aging.

The prediction of the complex moduli after long-term aging for the laboratory samples proved to be acceptable. The proposed methodology permits researchers to obtain the Aging Index of asphalt mixtures by combining the aging shift factor and the slopes of the master curves (the latter established for multiple periods). To that end, the AI predicts mastic behavior—and, in turn, asphalt mixture behavior—during the first 1000 hours of UV chamber exposure or 2 years of service life. In Colombian mastics, hardening may increase up to 180% of the average, where the initial complex modulus serves as the starting value. This study also demonstrates that filler content reduces hardening in soft asphalts (AC-80-100) more than in hard asphalts (AC-60-70).

Colombian AC-60-70 exhibits worse performance in terms of aging in spite of the fact that the master curves of the complex moduli are similar to those of AC-80-100. This conclusion was based on observations that AC-60-70's AI is greater than that of AC-80-100 when filler content is 20%, as is often the case in the field. However, aging in AC-80-100 tends to progress more rapidly throughout service life, given that the slopes of its master curves are greater. These increased slopes translate into more susceptibility to cracking after the first year of service life.

The AI values presented by the field samples after 6 years of service life are parallel to those obtained from laboratory samples subjected to 500 hours of UV chamber treatment. Consequently, we believe aging chamber studies should continue to be carried out, so that we may collect data to determine whether the hardening process is continuous or whether environmental conditions cause softening-hardening cycles that went undetected by the procedures used.

Acknowledgements

The authors would like to thank the Material Testing and Civil Engineering laboratories at the Pontificia Universidad Javeriana; their gracious help was invaluable to the research conducted. In addition, thanks must go to Concescol SA for providing the materials required to carry out our research. Lastly, the authors would like to thank Joe Wager for tidying up their English composition.

IntechOpen

Author details

Carlos Alfonso Cuadro Causil^{1*}, Wilmar Darío Fernández-Gómez²,
Jorge Iván Osorio Esquivel¹ and Fredy Alberto Reyes Lizcano³

¹ Pontificia Universidad Javeriana, Bogotá, Colombia

² Center for Sustainable Pavements and Materials, Universidad Distrital Francisco José de Caldas, Bogotá, Colombia

³ Centro de Estudios de Carreteras, Transportes y Afines, Pontificia Universidad Javeriana, Bogotá, Colombia

*Address all correspondence to: carloscuadro@gmail.com

IntechOpen

© 2019 The Author(s). Licensee IntechOpen. This chapter is distributed under the terms of the Creative Commons Attribution License (<http://creativecommons.org/licenses/by/3.0>), which permits unrestricted use, distribution, and reproduction in any medium, provided the original work is properly cited. 

References

- [1] Bianchetto H, Miró R, Pérez F. R. Resistencia al envejecimiento de las mezclas bituminosas en caliente: Beneficios y limitaciones de la incorporación de filleres comerciales. Primera parte: estudios en base al método UCL; 2006
- [2] Bell CA, Kliwer JE. Evaluating Aging of Asphalt Mixtures; 1995
- [3] Fernández-Gómez W, Rondón H, Reyes F. A review of asphalt and asphalt mixture aging. *Ingeniería e Investigación*. 2013;33(1):5-12
- [4] Gawel I, Baginska K. Effect of chemical nature on the susceptibility of asphalt to aging. *Petroleum Science and Technology*. 2004;22:1261-1271
- [5] Huang S-C, Zeng M. Characterization of aging effect on rheological properties of asphalt-filler systems. *International Journal of Pavement Engineering*. 2007;8(3):213-223
- [6] Bicerano J, Douglas JF, Brune DA. Model for the Viscosity of Particle Dispersions; 1999
- [7] Butt AA, Jelagin D, Tasdemir Y, Birgisson B. The effect of wax modification on the performance of mastic asphalt. *International Journal of Pavement Research and Technology*. 2010;3(2):86-95
- [8] Buttlar WG, Bozkurt D, Al-Khateeb GG, Waldhoff AS. Understanding asphalt mastic behavior through micromechanics. *Transportation Research Record Journal of the Transportation Research Board*. 1999;1681(1):157-169
- [9] Anderson DA, Goetz WH. Mechanical Behavior and Reinforcement of Mineral Filler-Asphalt Mixtures: Technical Paper; 1973
- [10] Cooley LA, Stroup-Gardinder M, Brown ER, Hanson DI, Fletcher MO. Characterization of asphalt-filler mortars with superpave binder tests. *Journal of the Association of Asphalt Paving Technologists*. 1998;67:42-66
- [11] Harris BM, Stuart KD. Analysis of mineral fillers and mastics used in stone matrix asphalt (with discussion and closure). *Journal of the Association of Asphalt Paving Technologists*. 1995;64:54-95
- [12] Huang B, Shu X, Chen X. Effects of mineral fillers on hot-mix asphalt laboratory-measured properties. *International Journal of Pavement Engineering*. 2007;8(1):1-9
- [13] Kallas BF, Puzinauskas VP. A study of mineral fillers in asphalt paving mixtures. In: *Proceedings, Association of Asphalt Paving Technologists*. 1961
- [14] Lesueur D, Little D. Effect of hydrated lime on rheology, fracture, and aging of bitumen. *Transportation Research Record Journal of the Transportation Research Board*. 1999;1661(1):93-105
- [15] Hopman P, Vanelstraete A, Verhasselt A, Walter D. Effects of hydrated lime on the behaviour of mastics and on their construction ageing. In: *Proceedings of the Durable and Safe Road Pavements, V International Conference*; 11-12 May 1999; Held Kielce, Poland. Vol. 1. 1999
- [16] Bahia HU, Anderson DA. The pressure aging vessel (PAV): A test to simulate reological changes due to field aging. In: *Phys. Prop. Asph. Cem. Bind*. 1995. pp. 67-88
- [17] Sisko AW, Brunstrum LC. Relation of Asphalt Rheological Properties to

Pavement Durability, NCHRP Rep. No. 67; 1967

[18] Dickinson EJ, Witt HP. The dynamic shear modulus of paving asphalts as a function of frequency. *Journal of Rheology*. 1974;18:591

[19] Anderson DA et al. Binder Characterization and Evaluation. Vol. 3: Physical Characterization; 1994

[20] Anderson DA, Christensen DW, Bahia H. Physical properties of asphalt cement and the development of performance-related specifications. *Journal of the Association of Asphalt Paving Technologists*. 1991;60:437-475

[21] Christensen DW, Anderson DA. Interpretation of dynamic mechanical test data for paving grade asphalt cements (with discussion). *Journal of the Association of Asphalt Paving Technologists*. 1992;61:67-116

[22] Jongepier R, Kuilman B, Schmidt RJ, Puzinauskas VP, Rostler FS. Characteristics of the rheology of bitumens. In: *Association of Asphalt Paving Technologists Proc*. 1969

[23] Dobson GR. On the development of rational specifications for the rheological properties of bitumens. *Journal of the Institute of Petroleum*. 1972;58(559):24

[24] Stastna J, De Kee D, Powley MB. Complex viscosity as a generalized response function. *Journal of Rheology*. 1985;29:457

[25] Marasteanu MO, Anderson DA. Improved model for bitumen rheological characterization. In: *Eurobitume Workshop on Performance Related Properties for Bituminous Binders*. 1999

[26] Zeng M, Bahia H, Zhai H, Turner P. Rheological modeling of modified asphalt binders and mixtures. *Asphalt Paving Technology*. 2001;70:403-441

[27] Mohammad LN, Wu Z, Myers L, Cooper S, Abadie C. A practical look at the simple performance tests: Louisiana's experience (with discussion). *Journal of the Association of Asphalt Paving Technologists*. 2005;74:557-600

[28] Huet C. Étude par une méthode d'impédance du comportement viscoélastique des matériaux hydrocarbures. Paris: Faculté des Sciences de Paris; 1963

[29] Sayegh G. Viscoelastic properties of bituminous mixtures. In: *Intl Conf Struct Design Asphalt Pvmnts*. 1967

[30] Olard F, Di Benedetto H. The "DBN" model: A thermo-visco-elasto-plastic approach for pavement behavior modeling (with discussion). *Journal of the Association of Asphalt Paving Technologists*. 2005;74:791-828

[31] Kim YR. Modeling of Asphalt Concrete. ASCE Press United State of America; 2009

[32] Yusoff NIM, Shaw MT, Airey GD. Modelling the linear viscoelastic rheological properties of bituminous binders. *Construction and Building Materials*. 2011;25(5):2171-2189

[33] Fernandez-Gomez W, Rondón H, Daza C, Fredy R. The effects of environmental aging on Colombian asphalts. *Fuel*. 2014;115:321-328

[34] Cuadro Causil CA, Osorio Esquivel JI. Construcción de las curvas maestras del Mástico a partir del análisis reológico de muestras elaboradas en laboratorio y de muestras recuperadas de mezclas en servicio; 2012

[35] McGreer M. Weathering Testing Guidebook. Atlas Material Testing Technology; 2003